

Momentum scale dependence of the net quark number fluctuations near chiral crossover

Kenji Morita^{1,2,*} and Krzysztof Redlich^{2,3}

¹*Yukawa Institute for Theoretical Physics, Kyoto University, Kyoto 606-8502, Japan*

²*Institute of Theoretical Physics, University of Wrocław, PL-50204 Wrocław, Poland*

³*Extreme Matter Institute EMMI, GSI, Planckstr. 1, D-64291 Darmstadt, Germany*

(Dated: December 9, 2019)

We investigate properties of the net baryon number fluctuations near chiral crossover in a hot and dense medium of strongly interacting quarks. The chirally invariant quark-antiquark interactions are modeled by an effective quark-meson Lagrangian. To preserve remnants of criticality in the $O(4)$ universality class, we apply the functional renormalization group method to describe thermodynamics near chiral crossover. Our studies are focused on the influence of the momentum cuts on the critical behavior of different cumulants of the net quark number fluctuations. We use the momentum scale dependence of the flow equation to examine how the suppression of the momentum modes in the infrared and ultraviolet regime modifies generic properties of fluctuations expected in the $O(4)$ universality class. We show, that the pion mass m_π is a natural soft momentum scale at which cumulants are saturated at their critical values, whereas for scales larger than $2m_\pi$ the characteristic $O(4)$ structure of the higher order cumulants get lost. These results indicate, that when measuring fluctuations of the net baryon number in heavy ion collisions to search for a partial restoration of chiral symmetry or critical point, a special care have to be made when introducing kinematical cuts on the fluctuation measurements.

PACS numbers: 25.75.Nq, 25.75.Gz, 24.60.-k, 12.39.Fe

I. INTRODUCTION

Exploring possible evidence of partial restoration of chiral symmetry in a medium created in heavy ion collisions is one of the most important and challenging problems [1–3]. Experimental studies along this line have been carried out by measuring fluctuations of conserved charges, in particular, of the net baryon number [4, 5] and the electric charge [6].

Fluctuations of conserved charges are particularly interesting probes of critical phenomena and phase diagram in QCD. The charge currents couple to the soft “sigma” modes, thus correlations and fluctuations of charge densities are directly affected by the chiral symmetry restoration at finite temperature and net baryon number density [7–12].

For massless two-flavor quarks, the QCD phase transition was conjectured to be of the second order, and belonging to the $O(4)$ universality class [13]. Current lattice QCD (LQCD) simulations at physical quark masses show, that at vanishing and small baryon density the transition from a hadron gas to a quark gluon plasma is crossover [14]. In addition, LQCD also indicates, that the chiral crossover appears in the critical region of the second order transition belonging to the $O(2)/O(4)$ universality class [15, 16]. Consequently, observables which are sensitive to criticality related with a spontaneous breaking of a chiral symmetry, in this fluctuations of net baryon number and electric charge, should exhibit char-

acteristic properties governed by the universal part of the free energy density [9, 10]. The magnetic equation of states and cumulants of net charges at physical quark masses have been studied in first principle lattice QCD calculations [17–20], as well as in effective chiral models [21–32]. Their properties which are obtained beyond mean-field level, have been shown to be consistent with general expectations originating from the $O(4)$ scaling.

The above results have opened new opportunity to verify the QCD phase boundary experimentally by measuring fluctuations of conserved charges [10, 16, 18, 28, 33–35], and their probability distributions [36–39]. This is particularly the case, since the chiral pseudocritical line appears near the phenomenological freezeout line [10]. Consequently, the hadron resonance gas partition function constitutes the regular part of a free energy density of QCD in a hadronic phase, thus also, a reference for the non-critical behavior of net charge fluctuations and their probability distribution at the phase boundary [10, 33, 37, 39].

Cumulants of net baryon number fluctuations, quantified by the net protons, have recently been explored in heavy ion collisions by STAR Collaboration [4, 5]. The data show deviations from the HRG reference, which are qualitatively consistent with theoretical expectations based on the $O(4)$ chiral critical dynamics [39]. However, the role of different approximations and uncertainties associated with the event-by-event measurements of fluctuations remains to be clarified [40–44].

In particular, STAR measurements of the Beam Energy Scan program at the Relativistic Heavy Ion Collider, were carried out at midrapidity and within the transverse momentum range $0.4 < p_T < 0.8$ GeV/c.

*Electronic address: kmorita@yukawa.kyoto-u.ac.jp

The criticality related with the chiral symmetry restoration is dominantly governed by soft momentum modes. Consequently, momentum cuts can implicitly influence properties of cumulants of conserved charges near phase boundary.

The main objectives of this paper is to study how the momentum cuts can modify critical properties of different cumulants of the net baryon number in the $O(4)$ universality class. Our studies are carried out within the quark-meson (QM) model. In order to correctly account for the $O(4)$ scaling properties of different physical observables near the chiral transition we apply the functional renormalization group (FRG) method [45–47].

We use the momentum scale dependence of the FRG flow equation [48–51] to examine how the suppression of the momentum modes in the infrared and ultraviolet regimes modifies generic properties of the net-baryon number fluctuations in the $O(4)$ universality class.

We show, that the pion mass m_π is a natural soft momentum scale at which cumulants are saturated at their critical values, whereas for scales larger than $2m_\pi$ the characteristic $O(4)$ structure of the higher order cumulants get lost. We also show, that the restriction of momentum modes in the ultraviolet regime can as well deflect the $O(4)$ structure of the net baryon number fluctuations.

Our results indicate, that when measuring fluctuations of the net baryon number in heavy ion collisions to search for partial restoration of the chiral symmetry or critical point, a detailed dependence of the results on kinematical cuts has to be examined.

This paper is organized as follows: in the next section, we introduce the quark-meson model and its critical properties. In Sec. III, we present results on momentum scale dependence of different cumulants and their ratios. Section IV is devoted to the concluding remarks.

II. QUARK-MESON MODEL AND FLUCTUATIONS

We employ the two-flavor quark-meson model to explore the momentum scale dependence of the net quark number fluctuations at finite temperature and density. The quark-meson model is an effective realization of low energy properties of QCD in which chiral symmetry breaking is described by $O(4)$ meson multiplet $\phi = (\sigma, \vec{\pi})$ coupled to quark fields q with Yukawa coupling constant g . The QM model Lagrangian reads

$$\mathcal{L} = \bar{q}[i\gamma_\mu \partial^\mu - g(\sigma + i\gamma_5 \vec{\tau} \cdot \vec{\pi})]q + \frac{1}{2}(\partial_\mu \sigma)^2 + \frac{1}{2}(\partial_\mu \vec{\pi})^2 - U(\sigma, \vec{\pi}), \quad (1)$$

where $U(\sigma, \vec{\pi})$ denotes the mesonic potential

$$U(\sigma, \vec{\pi}) = \frac{1}{2}m^2\phi^2 + \frac{\lambda}{4}\phi^4 - h\sigma. \quad (2)$$

The $O(4)$ chiral symmetry is spontaneously broken to $O(3)$ yielding $\langle \sigma \rangle \neq 0$ when $m^2 < 0$. The explicit symmetry breaking term $-h\sigma$ with $h = f_\pi m_\pi^2$ gives the nonzero pion mass.

A. Flow equation for quark-meson model at finite temperature and density

The functional renormalization group (FRG) approach provides an efficient method to evaluate the effective potential, which accounts for quantum fluctuations [45–47, 52].

We introduce a scale dependent effective action $\Gamma_k[\phi, q]$, which becomes the classical action S at the ultraviolet cutoff scale Λ , and the full quantum effective action $\Gamma[\phi, q]$ in the $k \rightarrow 0$ limit

$$\Gamma_\Lambda = S, \quad \Gamma_{k \rightarrow 0} = \Gamma. \quad (3)$$

The evolution of $\Gamma_k[\phi, q]$ with the renormalization scale k is given by the following flow equation [45]

$$\partial_k \Gamma_k[\phi, q] = -\text{Tr} \left[\partial_k R_{kF}(p)(R_{kF}(p) + \Gamma_k^{(2,0)})^{-1} \right] + \frac{1}{2} \text{Tr} \left[\partial_k R_{kB}(p)(R_{kB}(p) + \Gamma_k^{(0,2)})^{-1} \right], \quad (4)$$

where $\partial_k \equiv \partial/\partial k$, and the trace runs over the internal momentum p , as well as spinor, color and flavor indices. The $R_{k,B}(p)$ is an arbitrary cutoff function which suppresses propagations of the bosonic modes with $p < k$, originating from inserting a mass-like term, $\frac{1}{2} \int \frac{d^D p}{(2\pi)^D} R_{k,B}(p)\phi(p)\phi(-p)$, into the action. The fermionic counterpart, $R_{k,F}(p)$ is introduced in a similar fashion. The $\Gamma_k^{(a,b)}$ in Eq. (4), denotes the a -times fermionic and b -times bosonic functional derivatives of $\Gamma_k[\phi, q]$.

Owing to the scale dependent two-point functions, the flow equation (4) has the one-loop structure with an insertion of $\partial_k R_{k,B(F)}(p)$ which has a strong peak at $p = k$. At finite temperature, following the standard imaginary time formalism, the integral over the loop momentum p is replaced by a Matsubara sum.

To solve the flow equation, we employ the following optimized regulator functions [53]

$$R_{k,B}^{\text{opt}}(\mathbf{p}) = (k^2 - \mathbf{p}^2)\theta(k^2 - \mathbf{p}^2) \quad (5)$$

$$R_{k,F}^{\text{opt}}(\mathbf{p}) = (p + i\mu\gamma^0) \left(\sqrt{\frac{(p_0 + i\mu)^2 + k^2}{(p_0 + i\mu)^2 + \mathbf{p}^2}} - 1 \right) \theta(k^2 - \mathbf{p}^2) \quad (6)$$

In the integration over the internal momentum p , the cutoff functions $R_{k,B(F)}(p)$ in a full propagator plays a role of a mass below $p < k$, and its derivative $\partial_k R_k(p)$ implements an integration of momentum shell, as in an original Wilsonian idea. By integrating the flow equation

Eq. (4), from $k = \Lambda$ to $k \simeq 0$, one gets the full effective action, which includes quantum fluctuations.

The flow equation (4) for the scale dependent effective action, includes the two-point function. Formally one can obtain the flow equation for the scale-dependent two-point function by taking the functional derivatives with respect to the fields. As the FRG flow includes higher order correlation functions, the flow equation exhibits an infinite hierarchy, which one needs to truncate to solve it.

The evolution of the k -scale dependent quantities, the so-called RG trajectory, depends on the choice of the regulator R_k and how to truncate the hierarchy, by construction.

To investigate critical phenomena, which are governed by soft modes, it is convenient to assume, that the field $\phi(x)$ varies slowly. Then, one can put an ansatz for the scale dependent effective action, based on the derivative

expansion. To leading order, and ignoring field renormalization, the ansatz reads

$$\Gamma_k[\phi] = \int d^D x \left[U_k(\phi(x)) + \frac{1}{2}(\partial_\mu \phi(x))^2 \right], \quad (7)$$

which is called, the local potential approximation. This approximation together with the optimized cutoff function has been shown to produce the $O(4)$ criticality in the QM model [48]. Thus we expect that different regulators and truncation schemes result only in small quantitative difference.

Putting this ansatz and the regulator functions (5) to the flow equation (4), one obtains a differential equation for the effective potential U_k in a closed form. Introducing a field variable $\rho \equiv \phi^2/2 = (\sigma^2 + \vec{\pi}^2)/2$, the flow equation for the scale dependent thermodynamic potential density $\Omega_k = T\Gamma_k/V$ is given by

$$\partial_k \Omega_k(\rho; T, \mu) = \frac{k^4}{12\pi^2} \left[\frac{3}{E_\pi} \{1 + 2n_B(E_\pi)\} + \frac{1}{E_\sigma} \{1 + 2n_B(E_\sigma)\} - \frac{2\nu_q}{E_q} \{1 - n_F(E_q + \mu) - n_F(E_q - \mu)\} \right]. \quad (8)$$

The first, second, and third terms stand for π , σ , and quark contributions, as seen from the corresponding thermal distribution functions n_B and n_F with the quasiparticle energies $E_a = \sqrt{k^2 + m_{a,k}^2}$, where $a = \pi, \sigma$ or q . The scale dependent effective mass of mesons are related to the effective potential with the explicit breaking term being removed, $\bar{\Omega}_k = \Omega_k + h\sqrt{\rho_k}$,

$$m_{\pi,k}^2 = \Omega'_k \quad (9)$$

$$m_{\sigma,k}^2 = \bar{\Omega}'_k + 2\rho_k \bar{\Omega}''_k, \quad (10)$$

where $\bar{\Omega}'_k = \partial \bar{\Omega}_k / \partial \rho$. The dynamical quark mass is directly related to the order parameter

$$m_{q,k} = g\sigma_k, \quad (11)$$

where the Yukawa coupling $g = 3.2$ is fixed to get $m_{q,0} = 300\text{MeV}$ at $T = 0$.

The flow equation (8) is solved numerically with a Taylor expansion method [48] in which the scale dependent potential is expanded around its minimum ρ_k , up to the third order in ρ , as

$$\bar{\Omega}_k(\rho) = \sum_{n=0}^3 \frac{a_{n,k}}{n!} (\rho - \rho_k)^n. \quad (12)$$

The coefficients $a_{n,k}$, and the minimum ρ_k , follow the

following flow equations

$$\begin{aligned} d_k a_{0,k} &= \frac{h}{\sqrt{2\rho_k}} d_k \rho_k + \partial_k \Omega_k, \\ d_k \rho_k &= -\frac{1}{c/(2\rho_k)^{3/2} + a_{2,k}} \partial_k \Omega'_k, \\ d_k a_{2,k} &= a_{3,k} d_k \rho_k + \partial_k \Omega''_k, \\ d_k a_{3,k} &= \partial_k \Omega'''_k, \end{aligned} \quad (13)$$

where $d_k \equiv d/dk$, and $a_{1,k}$ is eliminated by making use of the scale independent relation $h \equiv a_{1,k} \sqrt{2\rho_k}$. The initial condition at an ultraviolet cutoff scale $\Lambda = 1.0 \text{ GeV}$ is chosen so as to satisfy the requirement (3), and to reproduce the vacuum physics. Therefore, we set $a_{3,\Lambda} = 0$, whereas $a_{2,\Lambda}$ and ρ_Λ are fixed such as to reproduce $\sigma_{k=0}(T = \mu = 0) = f_\pi = 93\text{MeV}$ and $m_\sigma = 640\text{MeV}$ with $m_\pi = 135\text{MeV}$. While $a_{0,\Lambda}$ gives a constant shift in thermodynamic potential density, the lack of contributions from degrees of freedom above the ultraviolet cutoff scale, causes an unphysical behavior in thermodynamic quantities at high temperature [25, 54]. Thus, we include such contribution by integrating the flow equation from $k = \infty$ to $k = \Lambda$ for a non-interacting massless quarks and gluons,

$$\begin{aligned} \partial_k \Omega_k^\Lambda(T, \mu) &= \frac{k^3}{12\pi^2} \{2(N_c^2 - 1)[1 + 2n_B(k)] \\ &\quad - \nu_q[1 - n_F(k + \mu) - n_F(k - \mu)]\}. \end{aligned} \quad (14)$$

The pressure of the system is then obtained as, $p(T, \mu) = -\Omega_{k \rightarrow 0}$.

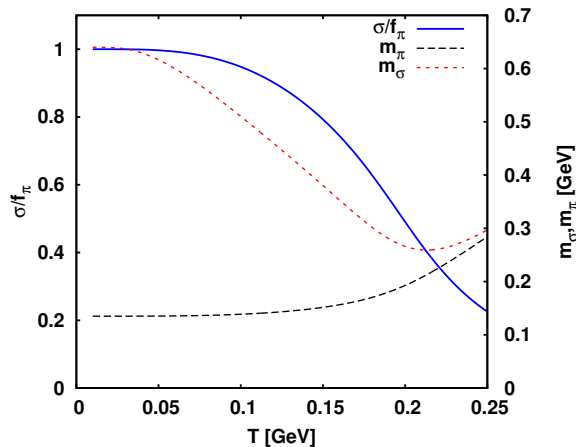


FIG. 1: The order parameter, the sigma and pion mass as a function of temperature, calculated in the quark-meson model within the functional renormalization group approach.

III. MOMENTUM SCALE AND CRITICALITY

A. Order parameter and meson masses

In the chiral limit, and at the moderate values of quark chemical potential, the QM model is well known to exhibit the second order phase transition in the $O(4)$ universality class which terminates at the critical end point, and then follows as the first order transition. For a physical pion mass the $O(4)$ phase transition is washed out and becomes a smooth crossover. Nevertheless, due to smallness of the light quark masses the crossover is constituted as the pseudocritical line along which the physical observables follow the scaling properties of the $O(4)$ universality class.

In the QM model, the order parameter of the chiral phase transition, is the expectation value of the σ -field. In Fig. 1, we show melting of the order parameter with temperature obtained by solving the flow equation (13). The chiral symmetry is spontaneously broken in a vacuum and is partially restored in a medium at some pseudocritical temperature $T = T_{pc}$. The values of T_{pc} for different quark chemical potential, can be identified as a peak position of the susceptibility of the order parameter or as the minimum of the sigma mass.

Figure 1 also shows the temperature dependence of the sigma and pion mass. The sigma mass is decreasing with temperature, whereas the pion mass is increasing towards T_{pc} , where it is approximately degenerate with the sigma mass. In the chiral limit the chiral condensate vanishes at the critical point where the sigma and the pion masses coincide.

The results shown in Fig. 1 were obtained within FRG approach, where all momentum modes up to $k = 0$ were integrated out, thus the thermal and quantum fluctuations have been included within the local potential approximation. However, the results of the RG-flow equa-

tions for the evolution of different physical observables with the infrared cutoff $k \neq 0$ can be also used to study the chiral symmetry breaking.

In Fig. 2-left, we show the momentum scale dependence of the order parameter, the pion and the sigma mass at $T = 0$. At large momentum scale $k \sim \Lambda$, the chiral symmetry is approximately valid, which is reflected in Fig. 2 by the small value of the order parameter and almost degenerate pion and sigma masses. When decreasing the scale below the ultraviolet cutoff Λ , there is a rapid growth of the order parameter towards its vacuum value. There is also a corresponding increase of the sigma mass after reaching a minimum at $k \sim k_{ch}$, where $k_{ch} \simeq 900$ MeV constitutes the momentum scale for an approximate chiral symmetry breaking.

The pion mass is seen in Fig. 2-left to decrease monotonically with decreasing momentum scale. On the other hand, the sigma mass is a non-monotonic function of k , as it reaches a maximum at $k \simeq 400$ MeV and then decreases towards the vacuum value. This property of sigma mass is consistent with previous finding in Ref. [55], and can be attributed to differences between the constituent quark and pion masses. A decrease of m_σ below $k < 400$ MeV is due to presence of the light pion.

At finite temperature, the scale dependence of the order parameter, the sigma and pion masses is qualitatively similar to the $T = 0$ case. In Fig. 2-right, we show the scale dependence of these observables at $T = T_{pc}$, where the chiral symmetry is partially restored. At large momenta $k \sim \Lambda$ the temperature effect is negligible. At lower scales, however, the thermal and meson fluctuations prevent the order parameter from growing to its vacuum value. The sigma mass and the order parameter reaches their maximum at $k \sim 600$ MeV, and then decrease towards values at the pseudocritical temperature. The pion exhibits a broad minimum at similar scale $k \sim 600$ MeV and then slightly increases towards $k = 0$.

Thus, it is clear that the RG-flow equations for the evolution with the infrared cutoff give a picture how the chiral criticality developed in a medium with the momentum scale. Clearly, to reproduce the expected $O(4)$ scaling of physical observables at the chiral crossover one needs the scale evolution towards $k = 0$. Any restriction on momentum scale in a medium modifies thermodynamically relevant information on universal properties.

To describe consequences of momentum scale cuts on the critical properties of relevant observables at the chiral crossover, we introduce the scale dependent ratios of such quantities calculated at the scale k and at $k = 0$. Figure 3 shows ratios for the order parameter, the pion and sigma masses at vanishing quark chemical potential and for two different vacuum pion masses. It is very transparent from Fig. 3, that at T_{pc} the natural momentum scale where these observables saturate at their critical values is the pion mass. This is seen by comparing the $m_\pi = 135$ and $m_\pi = 67.5$ MeV cases. One expects, that such a scale

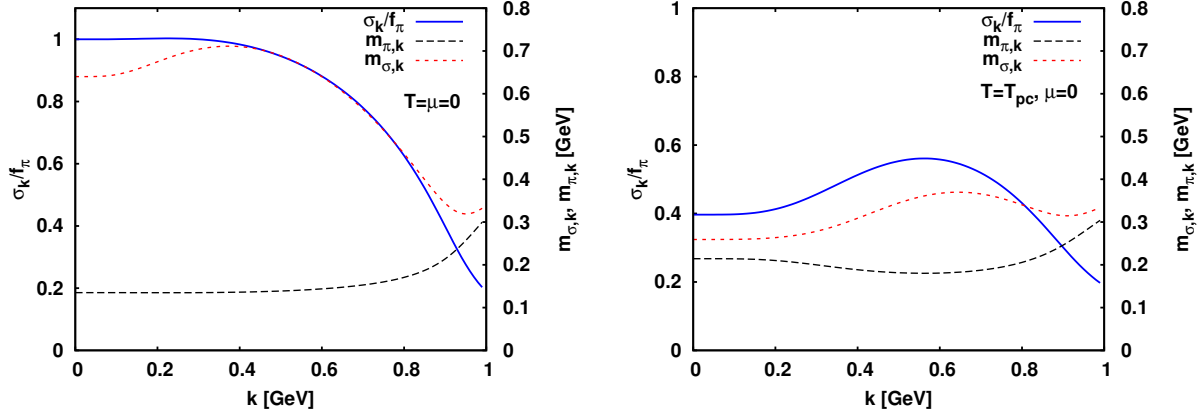


FIG. 2: The momentum scale dependence of the order parameter, the sigma and pion mass in the quark-meson model obtained from the renormalization group flow equation. The left-hand figure corresponds to $T = 0$ and the right-hand figure to $T = T_{pc}$, where T_{pc} is the pseudocritical temperature.

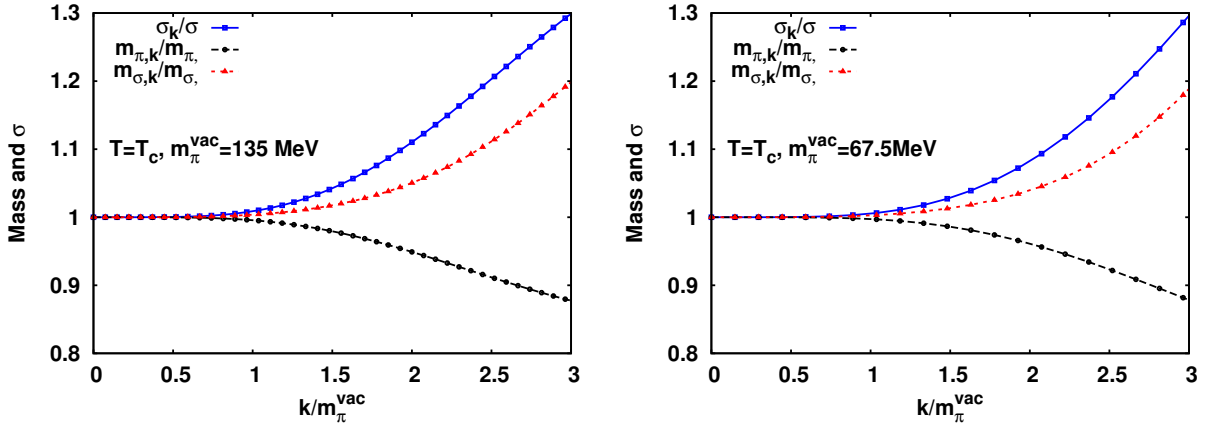


FIG. 3: As in Fig. 2-right, but the quantities are normalized to their values at $k = 0$ and the momentum scale is also normalized by the vacuum pion mass. The left-hand figure is calculated for the vacuum pion mass $m_\pi^{\text{vac}} = 135$ MeV, and the right-hand figure for $m_\pi^{\text{vac}} = 67.5$ MeV.

should be governed by the softest mode in a system.¹

Thus, if the momentum scale reaches $k \simeq m_\pi$, all these observables decouple from the RG flow. One can also conclude, that introducing any momentum cut in a system at $k \leq m_\pi$ will not modify relevant $O(4)$ properties near chiral crossover.

B. The net quark number fluctuations and momentum cuts

The sensitivity to the $O(4)$ criticality increases if the higher order fluctuations of the order parameter or conserved charges are considered at the chiral crossover. Of particular phenomenological interests are n th-order cumulants of the net quark number χ_n , which have been successfully quantified through the measurement of net proton number in heavy ion collisions by STAR Collaboration [4, 5]. Theoretically, the χ_n are obtained as derivatives of thermodynamic pressure with respect to the quark chemical potential,

$$\chi_n(T, \mu) \equiv \frac{\partial^n [p(T, \mu)/T^4]}{\partial (\mu/T)^n}. \quad (15)$$

In the vicinity of the chiral crossover, and due to remnants of the $O(4)$ criticality, the χ_n receive contributions

¹ In actual studies this is a quark mass m_q . However, this is not an observable and the critical behavior, *i.e.*, divergent fluctuations of conserved charges, is due to the mesonic sector since the light quark mass effect is already reflected in the mean field approximation.

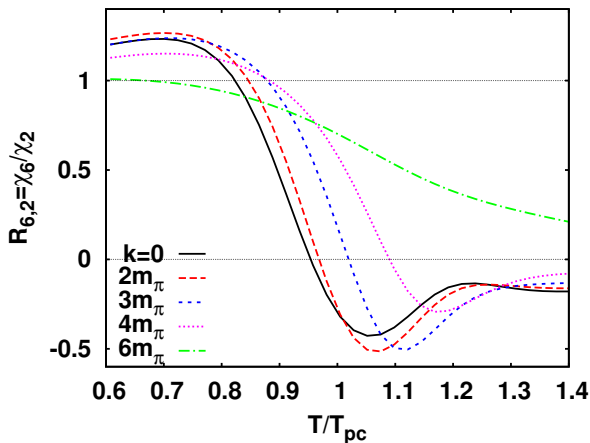


FIG. 4: The momentum scale dependence of the sixth to second order cumulant ratio in the quark-meson model calculated within the functional renormalization group method at finite temperature near the pseudocritical temperature T_{pc} . The momentum scales are expressed in units of a physical pion mass $m_\pi^{\text{vac}} = 135$ MeV.

from the regular and the singular part of the free energy density. Consequently, near T_{pc} one can decompose $\chi_n = \chi_n^s + \chi_n^r$, correspondingly. Owing to the $O(4)$ scaling, the χ_n^s show a strong dependence on the explicit symmetry breaking term h , the quark mass

$$\chi_n^s \sim \begin{cases} -h^{(2-\alpha-n/2)/\beta\delta} f_f^{(n/2)}(T, \mu) & \text{for } \mu = 0 \\ -\left(\frac{\mu}{T}\right)^n h^{(2-\alpha-n)/\beta\delta} f_f^{(n)}(T, \mu) & \text{for } \mu > 0, \end{cases} \quad (16)$$

where due to quark-antiquark symmetry at $\mu = 0$, the first equation holds only for even n . The α, β and δ are critical exponents in the $O(4)$ universality class, and $f^{(n)}$ is the n -th order derivative of the $O(4)$ universal scaling function with respect to the scaling variable [28, 56].

As $\alpha = -0.2131(34)$, is negative in the $O(4)$ universality class [56], the second and the fourth order cumulants of the net quark number fluctuations are finite in the chiral limit at the chiral transition temperature. From Eq. (16), it is clear, that at $\mu = 0$ the first divergent moment is obtained for $n = 6$, whereas at $\mu > 0$ for $n = 3$.

At fixed h , the T - and μ -dependence of χ_n^s is entirely governed by derivatives of the $O(4)$ universal scaling function. The characteristic feature of the sixth order cumulants at $\mu = 0$ is that at physical pion mass it can be negative near T_{pc} [28]. This makes χ_6 as an ideal observable of partial restoration of chiral symmetry in heavy ion collisions at RHIC and LHC if the chemical freezeout appears near the chiral crossover [10, 28].

Figure 4 shows the ratio $R_{6,2} = \chi_6 / \chi_2$ near T_{pc} at $\mu = 0$ calculated in the QM model. Since χ_2 is governed only by the regular part, the observed strong variation of $R_{6,2}$ and its negative structure, is entirely due to remnant of the $O(4)$ criticality in the sixth order cumulant. Thus, the expected generic structure of the $O(4)$ scal-

ing function in χ_6 is well reproduced in the QM model within FRG approach [28, 37], if the RG flow terminates at $k = 0$. Introducing the infrared momentum cutoff $k > 0$ can clearly deflect criticality near T_{pc} .

In Fig. 4, we show the $R_{6,2}$ by applying different infrared momentum cuts in units of the vacuum pion mass. The scale dependent net quark number fluctuations were calculated numerically as derivatives of the scale dependent thermodynamic potential density (8). With increasing momentum scale, the suppression of $R_{6,2}$ near T_{pc} due to $O(4)$ criticality is weakened. For sufficiently large momentum scale the characteristic negative structure of this fluctuation ratio disappears, indicating that the singular part contribution to χ_6 is suppressed. For $k > 5m_\pi$, the $R_{6,2}$ shows a smooth change from unity in the chirally broken phase to the value expected in the ideal massless quark gas. This indicates, that below T_{pc} and for large k , the structure of χ_6 is governed by the Skellam distribution, and that a smooth decrease of $R_{6,2}$ with T is due to decreasing quark mass with temperature and quantum statistics effect. However, if the momentum scale is smaller than $2m_\pi$, then a generic $O(4)$ structure of $R_{6,2}$ is preserved near T_{pc} . For $k > 2m_\pi$ the $R_{6,2}$ is not anymore negative in the chirally broken phase just below T_{pc} .

The change of $R_{6,2}$ with the infrared cutoff at the chiral crossover temperature T_{pc} is very transparent when considering the ratio of $R_{6,2}$ calculated at momentum scale k and that at $k = 0$. The corresponding results are shown in Fig. 5 for different vacuum pion masses. The pion mass fixes the scale where $R_{6,2}$ saturates at its critical value. Similarly to Fig. 2, if the infrared momentum scale reaches the softest mode which is approximately quantified by the pion mass, then the sixth order cumulant decouples from the RG flow. Figure 5 also indicates, that for $k < 2m_\pi$, the $R_{6,2}$ is weakly changing with infrared cutoff. Only for scales larger than $2m_\pi$, the $R_{6,2}$ at T_{pc} is positive, and the characteristic negative fluctuation due to $O(4)$ criticality is lost. At smaller pion mass $m_\pi \simeq 65$ MeV, the $R_{6,2}$ calculated up to $k = 0$ is positive at the T_{pc} .² This implies, that the normalized ratio shown in Fig. 5-right, increases with k for $k > 2m_\pi$.

In Fig. 5, the scale dependence of $R_{4,2}$ is also shown. Since at vanishing chemical potential, both χ_4 and χ_2 are non-critical at T_{pc} , $R_{4,2}$ is governed entirely by the regular part of the free energy. Consequently, $R_{4,2}$ is almost scale independent, as seen in this figure.

At finite chemical potential, already the third and higher order cumulants diverge at the chiral phase transition in the chiral limit. Consequently, for finite pion mass all χ_n with $n \geq 3$ are influenced by the $O(4)$ crit-

² The smaller pion mass is, the sharper crossover transition becomes. Thus $R_{6,2}$ also exhibits a sharper change around T_{pc} . The temperature where $R_{6,2} < 0$, shifts to higher values, since in the chiral limit $R_{6,2} > 0$ at $T < T_c$, and is positively or negatively divergent if $T \rightarrow T_c$ from below or above, respectively.

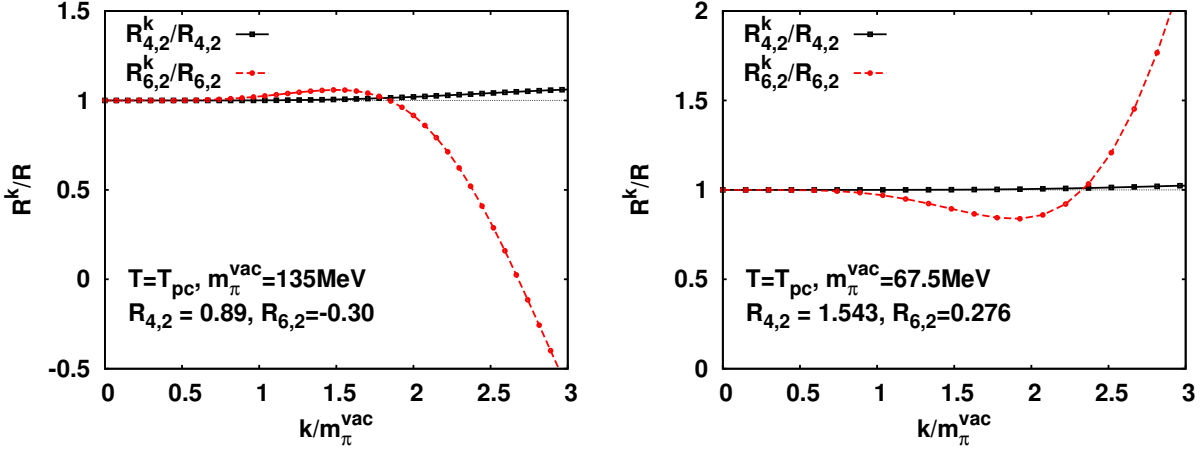


FIG. 5: The net quark number cumulants ratio $R_{n,m}^k = \chi_n/\chi_m$ at the pseudocritical point T_{pc} , calculated within the FRG method at the soft momentum scale k , and normalized to their value at the scale $k=0$, indicated in the figures. The left-hand figure is calculated for the vacuum pion mass $m_\pi^{\text{vac}} = 135$ MeV, and the right-hand figure for $m_\pi^{\text{vac}} = 67.5$ MeV.

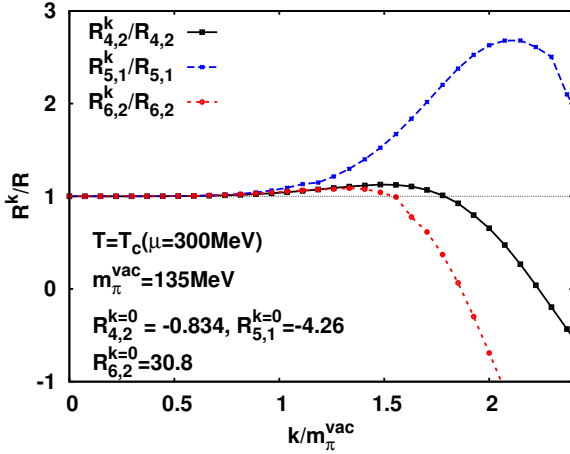


FIG. 6: As in Fig. 5-left, but the calculations are done at the pseudocritical temperature $T = 125\text{ MeV}$ for large finite quark chemical potential, $\mu_{pc} = 300$ MeV.

icality, thus should be also sensitive to the momentum scale at which they are calculated. In Fig. 6, we show ratios of $R_{n,m} = \chi_n/\chi_m$, calculated at momentum scale k and at $k=0$, for different orders of cumulant. These normalized ratios are evaluated at the chiral crossover point where the chemical potential is $\mu_{pc} = 300$ MeV and $T_{pc} = 125$ MeV. Similarly, as at $\mu = 0$, all $R_{n,m}$, shown in Fig. 6, saturate at their pseudocritical values if the momentum scale k reaches the pion mass. For scales $m_\pi < k < 1.5m_\pi$, deviations of $R_{3,1}$, $R_{4,2}$ and $R_{6,2}$ from their critical values are small. The $R_{5,1}$, however, exhibits much stronger scale dependence. Comparing the flow of $R_{6,2}$ at finite and vanishing μ , one concludes that at $\mu \neq 0$, there is a stronger sensitivity of this cumulants ratio to the soft momentum scale.

So far, effects of *infrared* momentum cut on the fluctuation observables have been discussed. Although, the criticality associated with partial restoration of chiral symmetry is governed by soft momentum modes, thus is related to the infrared cutoff, the ultraviolet cutoff also influences the fluctuations of the conserved charges.

Figure 7-left displays the temperature dependence of the cumulants ratios $R_{4,2}$ and $R_{6,2}$ with and without the ultraviolet cutoff $k_{\text{max}} = 0.8\text{ GeV}$. The calculation was done by setting the initial momentum scale to k_{max} without changing the vacuum physics, such that flow of the observables follow the same trajectory. The behavior of $R_{4,2}$ was already discussed in Ref. [25]. The absence of high momentum contribution implies, that χ_2 and χ_4 turn to decrease above T_{pc} , leading to suppression at high temperature. As seen in Fig. 7, $R_{6,2}$ follows the same trend.

Results employing, both infrared and ultraviolet cut-offs, $0.4 < k < 0.8$ GeV, are shown in Fig. 7-right. The effects of infrared and ultraviolet cutoffs on $R_{4,2}$, applied separately, were shown in Figs. 5 and 7-left to be small. Consequently, $R_{4,2}$ is seen in Fig. 7-right, to be also weakly sensitive if the momentum scales are constrained in both limits, simultaneously. However, the structure of $R_{6,2}$ is strongly changed. Its characteristic temperature dependence to the $O(4)$ criticality, represented by $R_{6,2}$ which is negative around T_{pc} and approaches to zero at high temperature, is lost. Instead, $R_{6,2}$ exhibits strong suppression to a larger negative values, due to the ultraviolet momentum cutoff.

The effects of momentum cuts are even stronger at finite chemical potential. Fig. 8 shows the $R_{4,2}$ as a function of temperature at $\mu = 300\text{ MeV}$ where $T_{pc} = 125$ MeV. Contrary to the case of $\mu = 0$, the cutoff changes the sign of $R_{4,2}$ near the chiral cross over. While the negative structure of $R_{4,2}$ at $T_{pc} = 125$ MeV signals the rem-

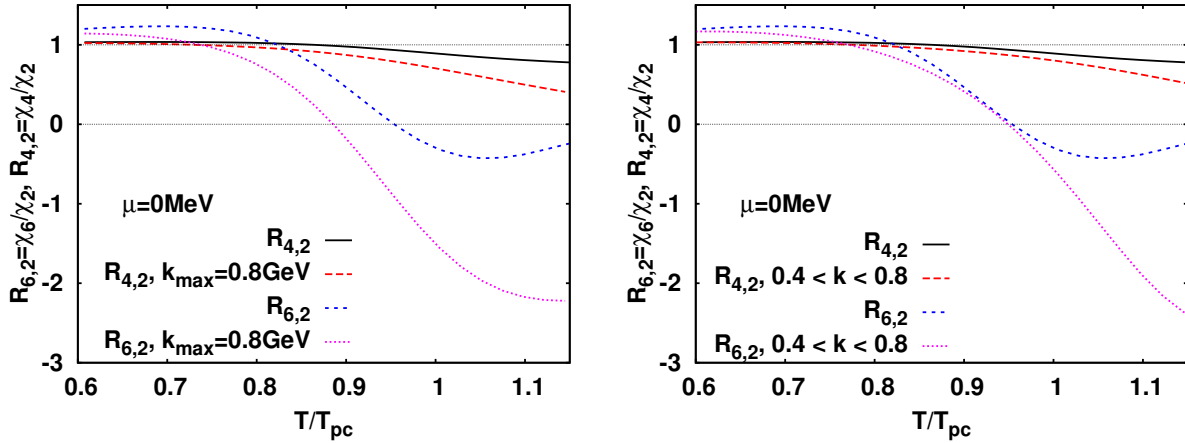


FIG. 7: Temperature dependence of the net quark number cumulants ratio, $R_{n,m} = \chi_n / \chi_m$. In the left hand figure: the $R_{n,m}$, calculated in the quark-meson model in the FRG flow within full momentum range is compared with the corresponding result with the ultraviolet momentum cut $k_{\text{max}} = 0.8$ GeV. In the right hand figure: the full FRG result for $R_{n,m}$ is compared with the corresponding result obtained in the momentum interval $0.4 < k < 0.8$ GeV.

nant of the $O(4)$ criticality, the infrared cutoff $k > 2.2m_\pi$ implies a changing the sign of $R_{4,2}$.

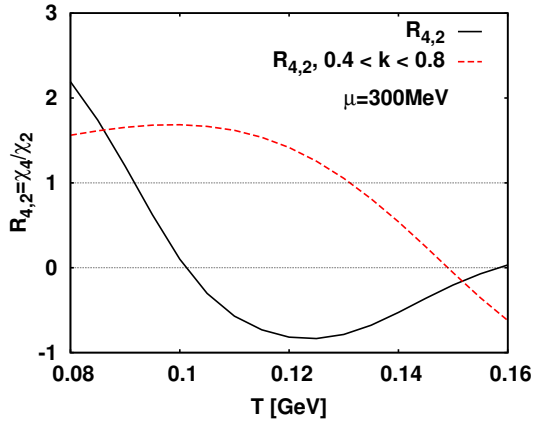


FIG. 8: As in Fig. 7-right but the calculations are done at fixed chemical potential $\mu = 300$ MeV.

Figures 7 and 8 make it clear, that imposing cutoffs in momentum scale, modifies the characteristic property of the cumulants ratio, which are specific to the chiral crossover at finite and vanishing chemical potential near the $O(4)$ pseudocritical points.

IV. CONCLUDING REMARKS

We have studied the momentum scale dependence of the net baryon number fluctuations near chiral crossover, which appear in the critical region of the second order phase transition in the $O(4)$ universality class. Our calculations were done in the quark-meson model within the

functional renormalization group (FRG) approach at finite and vanishing chemical potential. We have applied the momentum scale dependence of the FRG flow equation to quantify, how the suppression of the momentum modes in the infrared and ultraviolet regimes modifies generic properties of the net baryon number fluctuations ratio, expected from remnants of the $O(4)$ criticality.

We have shown, that the pion mass m_π is a natural infrared soft momentum scale at which cumulants are saturated at their critical values, whereas for scales larger than $2m_\pi$ the characteristic $O(4)$ structure of the higher order cumulants get lost.

In the ultraviolet regime, the momentum cutoff implies suppression of different cumulants ratios $R_{n,m}$. This suppression is small for $R_{n,m}$ which are insensitive to the chiral criticality. However, it is essential for ratios which are directly linked to the singular part of the free energy density, that is responsible for remnants of the $O(4)$ criticality in physical observables.

The above properties of different net baryon number cumulant ratios in a model with the $O(4)$ chiral critical behavior are in contrast to models with the Skellam probability distribution of the net baryon number, which is used as a reference for a non critical behavior. Imposing any momentum cutoffs in such models with Skellam function changes the values of different cumulants but preserves their ratios. These results indicate, that when measuring fluctuations of the net baryon number in heavy ion collisions to search for a restoration of a chiral symmetry or critical point, a special care have to be made when introducing kinematical cuts on the fluctuation measurements. In turn, this also implies, that one should observe modifications of the higher order cumulants ratios against the variation of the momentum cutoff, if they are influenced by the chiral critical behavior or its

remnant.

Acknowledgments

We acknowledge stimulating discussions with Bengt Friman and Chihiro Sasaki. This work was supported

by the Polish Science Foundation (NCN), under Maestro grant 2013/10/A/ST2/00106. K.M. was supported by the Grant-in-Aid for Scientific Research on Innovative Areas from MEXT (No. 24105008).

-
- [1] B. Friman, C. Höhne, J. Knoll, S. Leupold, J. Randrup, R. Rapp, and P. Senger, *Lect. Note. Phys.* **814**, 1 (2011).
 - [2] K. Fukushima and T. Hatsuda, *Rep. Prog. Phys.* **74**, 014001 (2011).
 - [3] K. Fukushima and C. Sasaki, *Prog. Part. Nucl. Phys.* **72** (2013) 99
 - [4] M. M. Aggarwal et al. (STAR Collaboration), *Phys. Rev. Lett.* **105**, 022302 (2010).
 - [5] L. Adamczyk et al. (STAR Collaboration), *Phys. Rev. Lett.* **112**, 032302 (2014).
 - [6] L. Adamczyk et al. (STAR Collaboration), *prl* **113**, 092301 (2014).
 - [7] Y. Hatta and M. A. Stephanov, *Phys. Rev. Lett.* **91**, 102003 (2003).
 - [8] M. Stephanov, K. Rajagopal, and E. Shuryak, *Phys. Rev. Lett.* **81**, 4816 (1998).
 - [9] S. Ejiri, F. Karsch, and K. Redlich, *Phys. Lett. B* **633**, 275 (2006).
 - [10] F. Karsch and K. Redlich, *Phys. Lett. B* **695**, 136 (2011).
 - [11] M. A. Stephanov, *Phys. Rev. Lett.* **102**, 032301 (2009).
 - [12] M. A. Stephanov, *Phys. Rev. Lett.* **107**, 052301 (2011).
 - [13] R. D. Pisarski and F. Wilczek, *Phys. Rev. D* **29**, 338 (1984).
 - [14] Y. Aoki, G. Endrödi, Z. Fodor, S. D. Katz, and K. K. Szabó, *Nature* **443**, 675 (2006).
 - [15] S. Ejiri, F. Karsch, E. Laermann, C. Miao, S. Mukherjee, P. Petreczky, C. Schmidt, W. Soeldner, and W. Unger, *Phys. Rev. D* **80**, 094505 (2009).
 - [16] O. Kaczmarek, F. Karsch, E. Laermann, C. Miao, S. Mukherjee, P. Petreczky, C. Schmidt, W. Soeldner, and W. Unger, *Phys. Rev. D* **83**, 014504 (2011).
 - [17] C. R. Allton, M. Döring, S. Ejiri, S. J. Hands, O. Kaczmarek, F. Karsch, E. Laermann, and K. Redlich, *Phys. Rev. D* **71**, 054508 (2005).
 - [18] A. Bazavov et al. (HotQCD Collaboration), *Phys. Rev. D* **86**, 034509 (2012).
 - [19] S. Borsanyi, Z. Fodor, S. D. Katz, S. Krieg, C. Ratti, and K. Szabo (Wuppertal-Budapest Collaboration), *JHEP* **1201**, 138 (2012).
 - [20] M. Cheng, P. Hedge, C. Jung, F. Karsch, O. Kaczmarek, E. Laermann, R. D. Nawhinney, C. Miao, P. Petreczky, C. Schmidt, et al., *Phys. Rev. D* **79**, 074505 (2009).
 - [21] K. Fukushima, *Phys. Lett. B* **591**, 277 (2004).
 - [22] C. Sasaki, B. Friman, and K. Redlich, *Phys. Rev. D* **75**, 054026 (2007).
 - [23] C. Sasaki, B. Friman, and K. Redlich, *Phys. Rev. D* **75**, 074013 (2007).
 - [24] B. Stokic, B. Friman, and K. Redlich, *Phys. Lett. B* **673**, 192 (2009).
 - [25] V. Skokov, B. Stokic, B. Friman, and K. Redlich, *Phys. Rev. C* **82**, 015206 (2010).
 - [26] V. Skokov, B. Friman, E. Nakano, K. Redlich, and B.-J. Schaefer, *Phys. Rev. D* **82**, 034029 (2010).
 - [27] V. Skokov, B. Friman, and K. Redlich, *Phys. Rev. C* **83**, 054904 (2011).
 - [28] B. Friman, F. Karsch, K. Redlich, and V. Skokov, *Eur. Phys. J. C* **71**, 1694 (2011).
 - [29] M. Asakawa, S. Ejiri, and M. Kitazawa, *Phys. Rev. Lett.* **103**, 262301 (2009).
 - [30] T. K. Herbst, J. M. Pawłowski, and B. J. Schaefer, *Phys. Lett. B* **696**, 58 (2011).
 - [31] B. J. Schaefer and M. Wagner, *Phys. Rev. D* **85**, 034027 (2012).
 - [32] M. Wagner, A. Walther, and B. J. Schaefer, *Comp. Phys. Comm.* **181**, 756 (2010).
 - [33] P. Braun-Munzinger, B. Friman, F. Karsch, K. Redlich, and V. Skokov, *Phys. Rev. C* **84**, 064911 (2011).
 - [34] A. Bazavov, H. T. Ding, P. Hegde, O. Kaczmarek, F. Karsch, E. Laermann, S. Mukherjee and P. Petreczky *et al.*, *Phys. Rev. Lett.* **109** (2012) 192302
 - [35] P. Braun-Munzinger, B. Friman, F. Karsch, K. Redlich, and V. Skokov, *Nucl. Phys.* **A880**, 48 (2012).
 - [36] K. Morita, V. Skokov, B. Friman, and K. Redlich, *Eur. Phys. J. C* **74**, 2706 (2014).
 - [37] K. Morita, B. Friman, K. Redlich, and V. Skokov, *Phys. Rev. C* **88**, 034903 (2013).
 - [38] A. Nakamura and K. Nagata, *arXiv:1305.0760*.
 - [39] K. Morita, B. Friman, and K. Redlich, *arXiv:1402.5982*.
 - [40] M. Kitazawa and M. Asakawa, *Phys. Rev. C* **85**, 021901 (2012).
 - [41] M. Kitazawa and M. Asakawa, *Phys. Rev. C* **86**, 024904 (2012).
 - [42] A. Bzdak and V. Koch, *Phys. Rev. C* **86**, 044904 (2012).
 - [43] A. Bzdak, V. Koch, and V. Skokov, *Phys. Rev. C* **87**, 014901 (2013).
 - [44] M. Nahrgang, M. Bluhm, P. Alba, R. Bellwied, and C. Ratti, *arXiv:1402.1238*.
 - [45] C. Wetterich, *Phys. Lett. B* **301**, 90 (1993).
 - [46] J. Berges, N. Tetradis, and C. Wetterich, *Phys. Rept.* **363**, 223 (2002).
 - [47] B. Delamotte, *arXiv:cond-mat/0702365*.
 - [48] B. Stokić, B. Friman, and K. Redlich, *Eur. Phys. J. C* **67**, 425 (2010).
 - [49] E. Nakano, B. J. Schaefer, B. Stokic, B. Friman, and K. Redlich, *Phys. Lett. B* **682**, 401 (2010).
 - [50] B. J. Schaefer and J. Wambach, *Phys. Rev. D* **75**, 085015 (2007).
 - [51] K. Kamikado, T. Kunihiro, K. Morita, and A. Ohnishi, *Prog. Theor. Exp. Phys.* **2013**, 053D01 (2013).
 - [52] H. Gies, *hep-ph/0611146*.
 - [53] D. Litim, *Phys. Rev. D* **64**, 105007 (2001).
 - [54] J. Braun, H. J. Pirner, and K. Schwenzer, *Phys. Rev. D* **70**, 085016 (2004).
 - [55] J. Braun, B. Klein, and H. J. Pirner, *Phys. Rev. D* **71**,

014032 (2005).

[56] J. Engels and F. Karsch, Phys. Rev. D **85**, 094506 (2012).